2016

Evidence of in Vivo Existence of Borrelia Biofilm in Borrelial Lymphocytomas

Eva Sapi
University of New Haven, ESapi@NewHaven.edu

Kunthavai Balasubramanian
University of New Haven

Akhila Poruri
University of New Haven

Jasmin S. Maghsoudlou
University of New Haven

Kayla Socarras
University of New Haven

See next page for additional authors

Publisher Citation

E. Sapi , K. Balasubramanian , A. Poruri , J. S. Maghsoudlou , K. M. Socarras , A. V. Timmaraju , K. R. Filush , K. Gupta , S. Shaikh , P. A. S. Theophilus , D. F. Luecke , A. MacDonald , B. Zelger (2016). Evidence of in vivo existence of Borrelia biofilm in borrelial lymphocytomas. European Journal of Microbiology and Immunology. Published online Feb. 9, 2016. doi: 10.1556/1886.2015.00049

Original article

European Journal of Microbiology and Immunology
DOI: 10.1556/1886.2015.00049

EVIDENCE OF *IN VIVO* EXISTENCE OF *BORRELIA* BIOFILM IN BORRELIAL LYMPHOCYTOMAS

E. Sapi[1,*], K. Balasubramanian[1], A. Poruri[1], J. S. Maghsoudlou[1], K. M. Socarras[1], A. V. Timmaraju[1], K. R. Filush[1], K. Gupta[1], S. Shaikh[1], P. A. S. Theophilus[1], D. F. Luecke[1], A. MacDonald[1], B. Zelger[2]

[1]Department of Biology and Environmental Science, University of New Haven, West Haven, CT 06516, USA
[2]Department of Dermatology and Venereology, Medical University Innsbruck, Innsbruck, Austria

Received: November 22, 2015; Accepted: December 2, 2015

Lyme borreliosis, caused by the spirochete *Borrelia burgdorferi sensu lato*, has grown into a major public health problem. We recently identified a novel morphological form of *B. burgdorferi*, called biofilm, a structure that is well known to be highly resistant to antibiotics. However, there is no evidence of the existence of *Borrelia* biofilm *in vivo*; therefore, the main goal of this study was to determine the presence of *Borrelia* biofilm in infected human skin tissues. Archived skin biopsy tissues from borrelial lymphocytomas (BL) were reexamined for the presence of *B. burgdorferi sensu lato* using *Borrelia*-specific immunohistochemical staining (IHC), fluorescent *in situ* hybridization, combined fluorescent *in situ* hybridization (FISH)–IHC, polymerase chain reaction (PCR), and fluorescent and atomic force microscopy methods. Our morphological and histological analyses showed that significant amounts of *Borrelia*-positive spirochetes and aggregates exist in the BL tissues. Analyzing structures positive for *Borrelia* showed that aggregates, but not spirochetes, expressed biofilm markers such as protective layers of different mucopolysaccharides, especially alginate. Atomic force microscopy revealed additional hallmark biofilm features of the *Borrelia*/alginate-positive aggregates such as inside channels and surface protrusions. In summary, this is the first study that demonstrates the presence of *Borrelia* biofilm in human infected skin tissues.

Keywords: Lyme disease, biofilm, mucopolysaccharides, alginate, atomic force microscopy

Abbreviations: AEC, 3-amino-9-ethylcarbazole; ATCC, American Type Culture Collection; AFM, atomic force microscopy; BL, borrelial lymphocytoma; BSA, bovine serum albumin; BSK-H, Barbour–Stoner–Kelly H; DAPI, 4′,6-diamidino-2-phenylindole; DIC, differential interference contract microscopy; EDTA, ethylenediaminetetraacetic acid; FAM, 6-fluorescein amidite; FFPE, formalin-fixed, paraffin-embedded; FISH, fluorescent *in situ* hybridization; FITC, fluorescein isothiocyanate; H&E, hematoxylin and eosin; IRB, Institutional Review Board; PBS, phosphate-buffered saline; PCR, polymerase chain reaction; RT, room temperature; SSC, saline sodium citrate

Introduction

Lyme disease**,** transmitted by the bite of infected ticks of the *Ixodes* genus, is an infectious disease caused by spirochetes belonging to the genus *Borrelia* [1]. Lyme disease is estimated to affect 300,000 people a year in the United States and 65,000 people per year in Europe [2].

Lyme disease patients are treated with various antibiotics though the rates of relapse and recurrence of the disease are frequent after discontinuing the antibiotic treatment [3–7]. It was proposed earlier that the observed antibiotic resistance and reoccurrence of Lyme disease might be due to the formation of defensive morphological forms of *Borrelia burgdorferi* [8–10].

In addition to its familiar spirochete form, *B. burgdorferi* can transform from motile spirochetes into round body forms in the presence of various unfavorable environmental conditions including the presence of antimicrobial agents [11–17]. The presence of those alternative forms was confirmed with numerous *in vitro* and *in vivo* studies; it was also proven that they respond to different antibiotic treatments than the spirochetal forms [18–22]. However, despite the fact that we might have good understanding about the effective treatment for those known alternative forms, *in vivo* studies still reported an uncultivable but infective form of *B. burgdorferi*, which could evade even the most aggressive antimicrobial treatments [23–26].

* Corresponding author: Eva Sapi; 300 Boston Post Road, West Haven CT 06516, USA; Phone: +1-203-479-4552, E-mail: esapi@newhaven.edu

Searching for potential answers for the observed high antibiotic resistance *in vivo*, we identified that this bacterium has an additional morphological form, called biofilm, a form which is very well known for allowing the bacteria to survive in adverse environmental conditions [27–31]. We provided evidence for the *in vitro* existence of borrelial biofilm using several known hallmark biofilm features including structural rearrangements in the aggregates producing a complex structure with channel and protrusions, a common feature in biofilm forming *Pseudomonas aeruginosa*, *Azotobacter vinelandii*, and *Leptospira biflexa* [32–37]. We also provided evidence that *B. burgdorferi sensu stricto* and *sensu lato* aggregates have specific surface biofilm markers such as alginate [30, 38], a mucopolysaccharide which is well characterized in biofilms of other pathogenic bacteria [39].

In addition, we and others have demonstrated that *B. burgdorferi* aggregate formation enhances the antibiotic resistance of the organism to various antibiotics, which previously showed some success against the spirochete and round body forms of *B. burgdorferi* [20–22, 40]. Taken together, these *in vitro* observations of biofilm formation suggest that *B. burgdorferi* could play significant role in their survival in diverse environmental conditions, by providing refuge to individual cells. However, the question remains if these structures can be found *in vivo* and whether these biofilm structures hold significant relevance for the survival strategies for *Borrelia* spp. in infected tissues.

In order to answer this question, we reexamined the findings from our earlier studies where we have seen similar *Borrelia* aggregates in infected skin tissues. We previously investigated different infected biopsy sections from known cutaneous complication of Lyme disease such as erythema chronicum migrans, borrelial lymphocytoma, and *Borrelia* acrodermatitis chronica atrophicans for the presence of *Borrelia*-positive structures [41]. We observed individual spirochetes in the sections as well as putative aggregates especially in the borrelial lymphocytoma (BL) tissues. These structures are strikingly similar to the ones we have previously seen and characterized in our *in vitro* culture systems that were proven to be biofilm [30].

Borrelial lymphocytoma, which develops weeks to months after the tick bite, is a rare but typical manifestation of Lyme disease found mainly in Europe [41, 42]. Because the low sensitivity of the available serology and molecular biology techniques, clinical diagnosis for BL still relies on clinical presentation and histological examination of the infected tissues [41, 42]. For example, histologic examination of cutaneous borrelial infections, including BL, usually reveals an infiltrate of lymphocytes, macrophages, and plasma cells in cutaneous lesions with "acral" predilection which are very characteristic of BL [41, 42].

Therefore, in this study, we used BL skin biopsies to evaluate whether the surface of *Borrelia*-positive aggregates could contain different mucopolysaccharides, especially alginate, to provide evidence for the existence of *Borrelia* biofilm *in vivo*. First, we used *Borrelia*-specific immunohistochemical (IHC), fluorescent *in situ* hybridization (FISH), and polymerase chain reaction (PCR) techniques to find *Borrelia* spirochetes and aggregates in the archived tissue biopsies from BL cases. We then further analyzed the surface of *Borrelia*-positive aggregates for potential mucopolysaccharides using different histological, IHC, combined IHC–FISH, and atomic force microscopy methods to further analyze those *Borrelia*/alginate-positive structures.

Materials and methods

Human tissue samples, processing biopsy specimens

From the files of our dermatohistopathologic laboratory, archived paraffin materials were retrieved from January 1975 to December 2005 from six cases of clinically confirmed borrelial lymphocytoma by certified dermatopathologists. All six cases had positive serology for *Borrelia* IgG, and characteristic features of borrelial lymphocytoma with "acral" predilection were found. All six patients were female (average age = 33 years) from endemic areas of Borreliosis in Austria with a rate of positive serology in the population between 30 and 60%. PCR confirmation for all six cases were performed independently in two different laboratories located in Austria and the US. The archival hematoxylin and eosin (H&E)-stained sections were reexamined, and the previous diagnosis also confirmed by two of us (B.Z. and A.M.D.). Institutional Review Board (IRB) exemption for this study was obtained from University of New Haven.

The paraffin blocks were sectioned by McClain Laboratories LLC (Smithtown NY) at 4 μm on TRUBOND200 adhesive slides. The sections then were deparaffinized by washing the sections three times in 100% xylene for 5 min each followed by rehydration in a series of graded alcohols (100%, 90%, and 70%) and washed in 1× phosphate-buffered saline (PBS) pH 7.4 for 5 min. For the immunohistochemical experiments, the tissues were incubated in 10 mM sodium citrate buffer for 45 min at 95 °C for antibody retrieval for the immunohistochemical experiments. For silver penetration method, the modified Dieterle method was used by the McClain Histopathology Laboratories LLC (Smithtown NY) following a previously published procedure by Duray P. et al. [43].

Bacterial cultures

Low passage isolates (<p3) of B. burgdorferi B31 (ATCC no. 35210), Borrelia garinii (ATCC no. 51991), Borrelia afzelii (ATCC no. 51992), and Treponema denticola (ATCC no. 33520) were obtained from American Type Culture Collection (ATCC). Borrelia hermsii was received from Dr. Tom G. Schwan's laboratory at Rocky Mountain Laboratories, NIH. Cells were maintained in Barbour–Stoner–Kelly H (BSK-H, Sigma) media supplemented with 6% or 12% (for T. denticola and B. hermsii) rabbit serum

(Pel-Freeze) without antibiotics in sterile 15 ml glass tubes and incubated at 33 °C with 5% CO_2. *Escherichia coli* biofilm forming strain was obtained from ATCC (ATCC no. 25922) and cultured overnight at 37 °C with shaking at 200 rpm in sterile 50 ml centrifuge tubes containing Luria broth media (Difco).

Slide preparation for in vitro *experiments*

Cell concentrations were determined using the Petroff-Hausser counting chamber method. A total of 1×10^6 cells per milliliter were centrifuged at 4000×*g* for 10 min at room temperature (RT) to remove the media. The supernatant was discarded, pellet was washed two times with 1 ml of 1× PBS (pH 7.4) and then resuspended in 100 µl of 1× PBS (pH 7.4), and the samples were smeared onto glass microscope slides (Superfrost+, Thermo Scientific). The smear was allowed to completely dry in a laminar airflow chamber, followed by fixation with ice-cold acetone for 15 min. Slides were then washed twice with 1× PBS (pH 7.4) at RT and used for the experiments.

Immunohistochemistry methods (IHC)

Two independent immunohistochemistry methods were performed as described before [30, 41]. Initially, the archived BL biopsy samples were immunostained with *Borrelia*-specific antibody to confirm the presence of *Borrelia* spp. in Innsbruck Medical University, utilizing the Ventana-KIT (Ventana Medical Systems, Munich, Germany). In this method, a biotinylated secondary antibody and a third layer of streptavidin–biotin horseradish peroxidase complex were utilized. As a final reaction product, 3-amino-9-ethylcarbazole (AEC) was used with bright red which proved to be superior to the brown diaminobenzidine. Negative control experiments were performed by omitting the primary antibody in an otherwise identical immunohistochemical procedure.

To further confirm the presence of *Borrelia* spp. in these tissues, the immunostaining was repeated at the University of New Haven using a previously published immunofluorescence protocol [30]. The *Borrelia*–alginate double staining IHC was performed in two different ways. On the same slides using the primary antibodies sequentially or consecutive slides using the two primary antibodies in parallel to provide information whether the two primary antibodies would have cross-reaction with the corresponding secondary antibodies. On the same slide method, the deparaffinized BL sections were first blocked with 10% normal goat serum (Thermo Scientific) in 1× PBS pH (7.4) for 30 min at RT to block nonspecific binding of the secondary antibody. The slides were then washed two times with PBS/0.5% bovine serum albumin (BSA) for 5 min each and further incubated at 37 °C for 1 h with fluorescein isothiocyanate (FITC)-labeled *Borrelia*-specific polyclonal antibody (#73005 Thermo Scientific, diluted 1:50 in 1× PBS/0.5% BSA). The slides were washed with 1× PBS five times for 5 min each at RT and counterstained with Sudan black (Sigma) and/or 4′,6-diamidino-2-phenylindole (DAPI) for 10 min. The slides were washed again with 1× PBS for 5 min, dried and mounted with PermaFluor aqueous mounting medium (Thermo Scientific). Images were acquired by fluorescent microscopy (Leica DM2500). On immunostaining method on sequential slides, the two primary antibodies were used in parallel experiment. For the IHC, two additional negative controls were used: 1) omitting primary antibody (use only 1× PBS + 0.5% BSA) and 2) normal human foreskin samples purchased commercially.

Spicer & Meyer mucopolysaccharide staining

The staining was performed as described previously with minor modifications [30]. Briefly, *Borrelia* aggregates on the deparaffinized and hydrated BL biopsy sections were stained with aldehyde fuchsine solution (Sigma-Aldrich, 0.5% fuchsine dye, 6% acetaldehyde in 70% ethanol with 1% concentrated hydrochloric acid) for 20 min. After immersing the slides in 70% ethanol for 1 min and having it rinsed with double-distilled water for another minute, the aggregates were sequentially stained with 1% Alcian blue 8GX (Sigma-Aldrich, dissolved in 3% acetic acid, pH 2.5) for 30 min. The slides were rinsed with double distilled water for 3 min and dehydrated using chilled graded ethanol washes (50%, 70%, and 95%, 3 min each). The slides were then immersed in chilled xylene for 2 min and mounted with Permount media (Fisher Scientific). Images were analyzed using different microscopy methods (see Results section).

Genomic DNA extraction

Genomic DNA was extracted from *B. afzelii* BO23 laboratory strain (ATCC no. 51992) using Qiagen DNeasy Blood and Tissue Kit (Qiagen) according to the manufacturer's instructions. All samples were stored at −20 °C until analysis. Genomic DNA from paraffin-embedded tissues fixed on glass slides was extracted using the Qiagen QIAamp DNA Formalin-fixed, Paraffin-Embedded (FFPE) Tissue Kit (Qiagen). First, the slides were deparaffinized, and then any tissues present on the slides were scraped off using sterile blades and collected in sterile microcentrifuge tubes. One hundred eighty microliters of ATL buffer and 20 µl of proteinase K were added to the tubes, and the samples were incubated overnight at 42 °C and then at 90 °C for 1 h to deactivate the enzyme. Two hundred microliters of AL buffer and an additional 200 µl of 96% ethanol were added to the samples and vortexed thoroughly. The samples were then transferred to DNeasy mini columns and centrifuged for 1 min at 6000×*g*. The flow-through was discarded, and the columns were placed into new collection tubes. To wash away any unwanted materials

that might be present along with the DNA, 500 µl of AW1 and AW2 buffers was added to the columns consecutively and centrifuged at 6000×*g* for 1 min. The spin columns were placed then in fresh collection tubes and centrifuged at 20,000×*g* for 3 min to completely dry the column. The columns were then placed in new microcentrifuge tubes, and the samples were eluted twice with 50 µl of ATE buffer. The samples were quantified using BioTek Microplate Spectrophotometer (BioTek) and stored at −20 °C until analysis.

PCR/DNA sequencing

PCR reactions were performed using primers designed to amplify *B. burgdorferi sensu lato* 16S ribosomal RNA small subunit. The 16S rRNA gene was amplified in a single reaction using primers F: 5′-CCTGGCTTAGAACTA-ACG-3′ and R: 5′-CCTACAAAGCTTATTCCTCAT-3′ in a 50-µl reaction containing HotStarTaq buffer (Qiagen) 1.5 mM $MgCl_2$, 25 pmoles of each primer, and 2.5 units of HotStarTaq DNA polymerase (Qiagen). The PCR reaction consisted of an initial denaturation at 94 °C for 15 min, followed by 40 cycles of 94 °C/30 s, 50 °C/30 s, 72 °C/1 min, and then a final extension at 72 °C/5 min. The PCR products were analyzed by standard agarose gel electrophoresis. PCR products were purified using the QIAquick PCR purification kit (Qiagen) according to the manufacturer's instructions. Samples were eluted twice in 30 µl, and the eluates from each sample were pooled and sequenced in both directions twice (4× coverage) using the same primers that generated the products. All DNA sequencings were performed by Eurofins/MGW/Operon (Huntsville, AL).

Fluorescent in situ *hybridization (FISH)*

A 32-base-long oligonucleotide probe was designed for *B. burgdorferi sensu lato* species-specific 16S ribosomal DNA (5′-GGATATAGTTAGAGATAATTATTCCCC-GTTTG-3′). The probe was designed to hybridize with *B. burgdorferi*, *B. garinii*, and *B. afzelii*, but not with *T. denticola* and *E. coli* strains (see validation study below). As a negative control, a 32-base-long random oligonucleotide probe (5′-GCATAGACATGAGATATACTGTACTAG-3′) was also designed. Both probes were synthesized and labeled with 6-fluorescein amidite (FAM) at the 5′ end by Eurofins MWG Operon oligonucleotide services. *In situ* hybridization probes were prepared by mixing 100 ng of labeled oligonucleotide with 2.5 µg salmon sperm DNA (Life Technologies) plus with 0.1 volume 3M sodium acetate (Fisher Scientific) and 2 volumes of ice cold ethanol, and the mixture was allowed to precipitate at −80 °C for 1 h. Probes were then centrifuged at 14,000 rpm for 20 min and resuspended in 10 µl hybridization buffer (50% *v*/*v* formamide [Sigma], 10% *w*/*v* dextran sulfate [Sigma], 1% *v*/*v* Triton X-100 [Sigma], and 2× saline sodium citrate [SSC] pH 7.0). Probes were then warmed to RT for 10 min, denatured at 95 °C for 10 min, and immediately cooled on ice for 10 min. Slides containing fixed cells were denatured in denaturing solution (70% *v*/*v* formamide, 2× SSC, 0.1 mM ethylenediaminetetraacetic acid [EDTA] pH 7.0) at 70 °C for 5 min and washed twice with cold 2× SSC followed by dehydration through a series of cold alcohol washes (70%, 90%, 100%). The sections were hybridized with the probe in the dark at 48 °C for 24 h. After hybridization, slides were washed three times with 2× SSC for 3 min each at RT followed by two 20 min washes in 0.1× SSC at 42 °C and a final wash in 0.1× SSC at RT. Finally, slides were blocked with freshly made blocking solution (3% *w*/*v* BSA [Fisher] in 4× SSC, 0.1% *v*/*v* Triton X-100) for 3 min and washed with a wash solution (4× SSC, 0.1 % *v*/*v* Triton X-100) for 3 min at room temperature.

For the paraffin-embedded tissue sections, the slides were first deparaffinized by heating on a slide warmer for 40 min at 45 °C and immersed in 100% xylene for 5 min three times. The slides were rehydrated in series of graded alcohols (100%, 90%, and 70%) and washed in PBS for 5 min and in distilled water for 15 min to rehydrate the tissues. The slides were treated with 4% sodium borohydride (Sigma-Aldrich) for 20 min on ice. The tissues were digested with prewarmed proteinase K solution (20 µg/ml in 50 mM Tris) for 10 min at 37 °C and refixed with 4% paraformaldehyde for 10 min at room temperature. The slides were denatured using preheated denaturing buffer (70% *v*/*v* formamide, 2× SSC, and 0.1 mM EDTA [Fisher] pH 7) at 70 °C followed by prehybridization for 4 h in hybridization buffer (50% *v*/*v* formamide [Sigma], 10% *w*/*v* dextran sulfate [Sigma], 1% *v*/*v* Triton X-100 [Sigma], 2× SSC, [Sigma] pH 7.0, and 2 ng of salmon sperm DNA) in an incubator at 48 °C. The sections were hybridized with the probe at 48 °C for 18 h in dark. After hybridization, slides were washed three times with 2× SSC for 3 min each at room temperature followed by five 20 min washes in 0.1× SSC at 42 °C and a final wash in 2× SSC at room temperature. Finally, slides were blocked with freshly made blocking solution (3% *w*/*v* BSA [Fisher] in 4× SSC, 0.1% *v*/*v* Triton X-100) for 30 min and washed with wash solution (4× SSC, 0.1 % *v*/*v* Triton X-100) for 3 min at room temperature. All steps were repeated with several controls such as: 1) 100 ng negative control random oligonucleotide, 2) 200 ng of unlabeled competing oligonucleotide present during the hybridization, and 3) following a DNase treatment of the sections before the hybridization step to digest all genomic DNA (100 µg/ml for 60 min at 37 °C). All slides were then analyzed by fluorescent microscopy using a Leica DM2500 biomedical microscope.

Combined FISH and IHC analyses

For the paraffin-embedded tissue sections, slides were first deparaffinized, rehydrated, and pretreated, and *in situ* hybridization protocol was followed as described above in the FISH section. After the last 0.2× SSC wash, the

sections were blocked with a 1:100 dilution of goat serum (Thermo Scientific) in 1× PBS pH 7.4 (Sigma) for 30 min at room temperature in a humidified chamber. The sections were then washed twice in 1× PBS (Sigma) for 5 min. Slides were then treated with a 1:500 dilution of primary anti-alginate antibody (provided by Dr. Gerald Pier, Harvard Medical School) in 1× PBS and placed in a humidified chamber overnight at room temperature and then washed twice in 1× PBS for 5 min and in distilled water for 5 min. Slides were then treated with a 1:200 dilution of a secondary anti-rabbit antibody with a fluorescent blue tag (405 nm, Thermo Scientific) for 1 h in a humidified chamber at room temperature. The sections were then washed twice in 1× PBS for 5 min and in distilled water for 5 min. Sections were then washed in 0.2× SSC for 5 min in the dark at room temperature. Sections were then counterstained with Sudan Black (Sigma) for 20 min. Sections were mounted with PermaFluor (Thermo Scientific), and images were captured using a Leica DM2500 fluorescent microscope. As a negative control, all steps were repeated with 200 ng of competing unlabeled oligonucleotide present during the hybridization.

Atomic force microscopy

The *Borrelia*/alginate-positive structures were visualized at nanometer-scale resolution through atomic force microscopy (AFM) analyses. First, the biopsy section was hydrated overnight at RT with 1× PBS (pH 7.4) buffer and rinsed with double distilled water two times before the scan. AFM scans on BL tissues were performed in contact mode using the Nanosurf Easyscan 2 AFM (Nanosurf) with SHOCONG probe (AppNANO™). Images were taken by Hamamatsu ORCA Digital Camera. Images were processed, and measurements were obtained using Gwyddion software.

Statistical analysis

Statistical analysis was performed using Student's *t*-test (Microsoft Excel, Redmond, WA) on the number of observed spirochetes and aggregates found in the 200 sections of the six BL specimens. Statistical significance was determined based on p value <0.05.

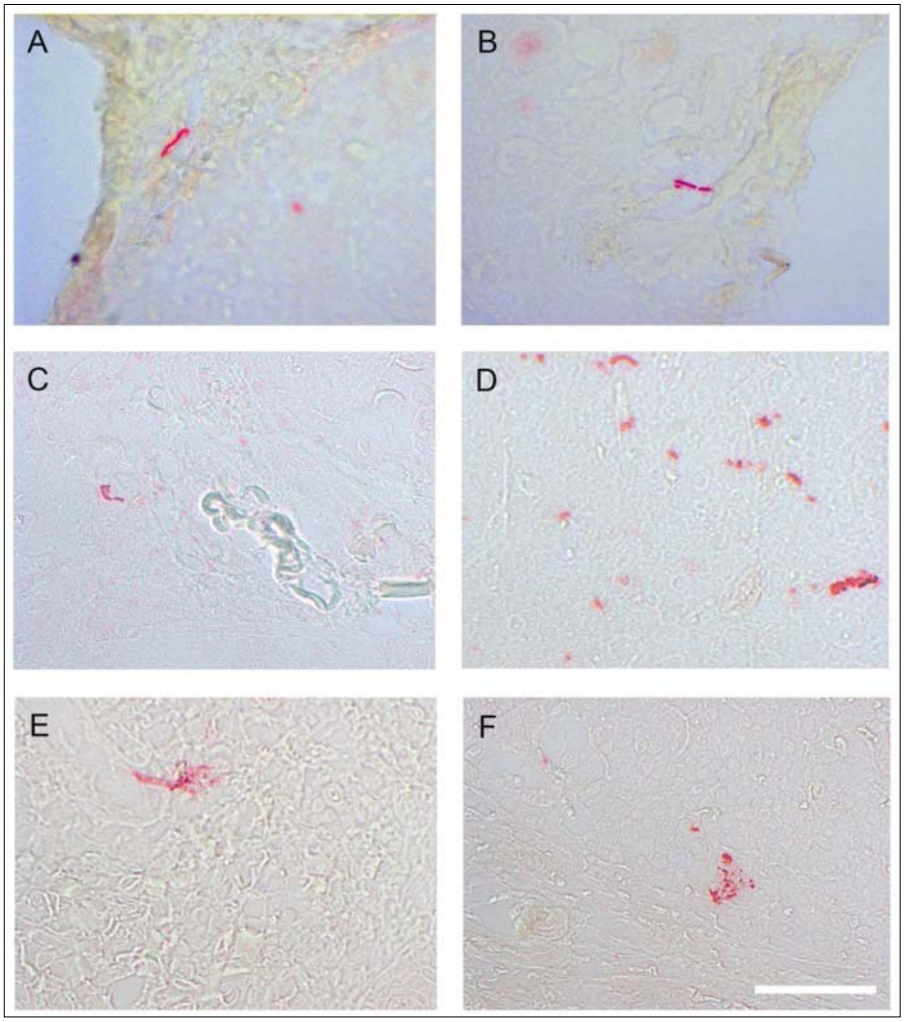

Fig. 1. Representative immunohistochemical (IHC) images of borrelial lymphocytoma (BL) tissue sections stained with *Borrelia*-specific antibody following an IHC protocol as described earlier [41]. Positive *Borrelia* staining is depicted by red color. 200× magnification, bar: 100 µm

Results

Presence of Borrelia *spirochetes and aggregates in BL tissues sections*

The overall goal of this study was to reexamine cutaneous cases of BL tissues to examine the potential presence of *Borrelia* biofilms *in vivo.* First, six cases of borrelial lymphocytoma archived tissues were retrieved from the files of our Dermatohistopathologic Laboratory in the Department of Dermatology and Venereology, Medical University Innsbruck. Archival H&E-stained sections were reexamined, and previous diagnoses were confirmed by two of us (B.Z. and A.M.D.). The presence of *Borrelia* was confirmed independently by two previously published immunohistochemical methods [41] in Medical University Innsbruck (Innsbruck, Austria) and in University of New Haven (West Haven, CT) combined with silver staining method performed in McClain Laboratory (Long Island, NY). *Figure 1* shows the representative images of the immunohistochemistry results of the six BL cases performed in Medical University Innsbruck. In all BL cases, the presence of *Borrelia* spirochetes and aggregates was clearly visible (red staining). *Figure 1E and F* show the presence of *Borrelia*-positive aggregates which were the subject for our further studies.

To further confirm the presence of *Borrelia* in the BL tissues, modified Dieterle method silver staining techniques were performed independently in McClain histopathology laboratories (Smithtown, NY). *Figure 2A* shows representative images of silver staining results on the BL tissues sections demonstrating silver stain positive spirochetal structures (*Fig. 2*, panels Ai and iv) as well as different sizes of silver-stained positive aggregates (*Fig. 2*, panels Aii and iii).

Aggregates which were positive for silver staining were then subjected to additional studies by immunostaining at the University of New Haven (West Haven CT, USA) of the consecutive sections with a different *Borrelia*-specific antibody to confirm that they are borrelial aggregates. *Figure 2B* shows that a silver-stained structure (can be found in both panel Aiii and panel Bv), but not the "no antibody" control (*Fig. 2*, panel Bvii), indeed stained positively with *Borrelia* antibody (*Fig. 2*, panel Bvi, green fluorescent

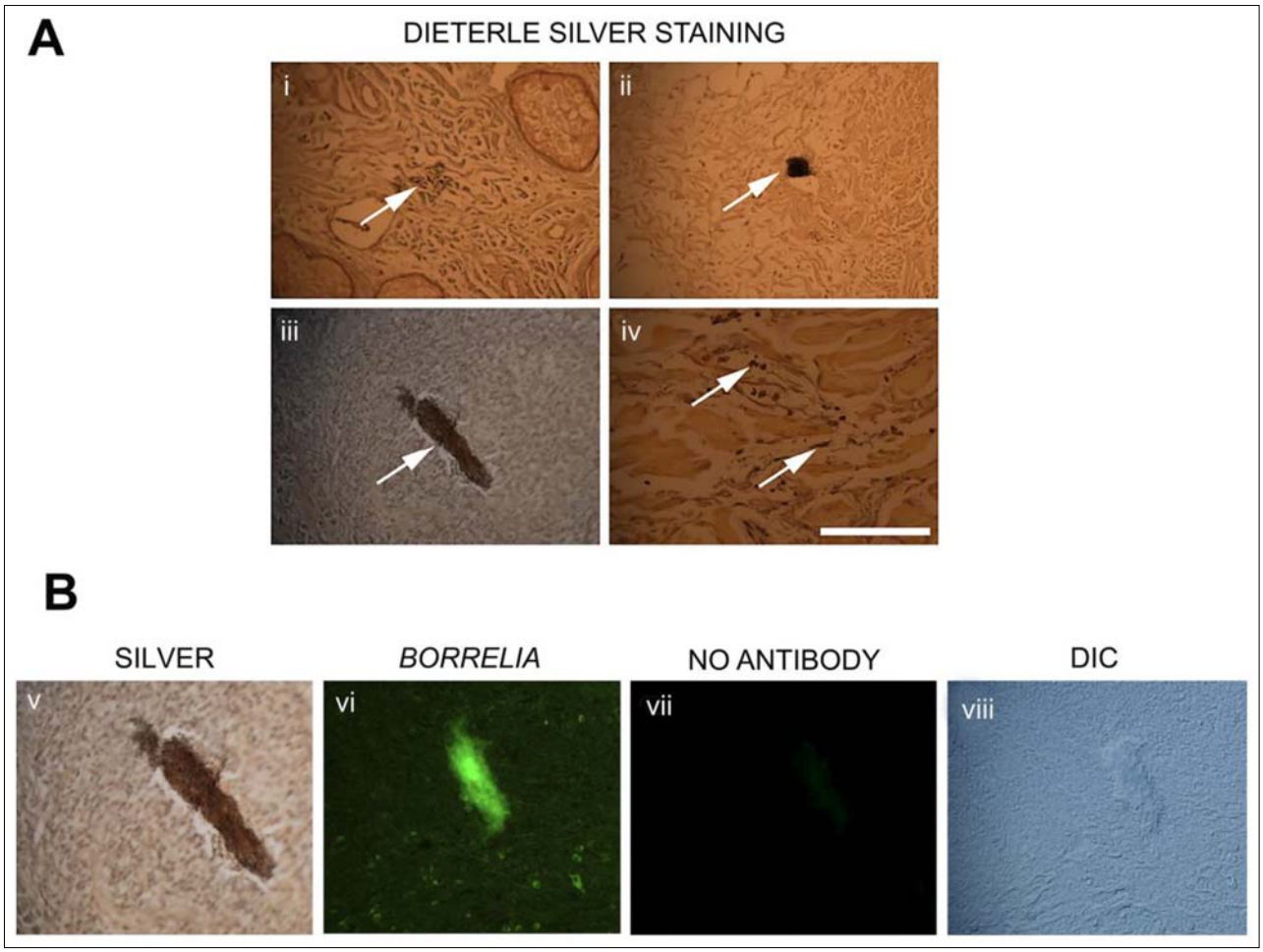

Fig. 2. Representative images of borrelial lymphocytoma (BL) tissue sections stained with modified Dieterle silver methods and *Borrelia*-specific IHC methods as described earlier [30]. White arrows in panel A show the silver-stained spirochetes (i and iv) and aggregates (ii and iii), and panel B shows one of the silver-stained aggregates (panel Aiii) stained positive for *Borrelia* antigen. As a negative control for the immunohistochemical method, panel Bvii shows a no antibody control on consecutive section, and panel Bviii is the DIC image of the panel Bvii section to prove that there is still aggregate on the tissue section. 400× magnification, bar: 200 μm

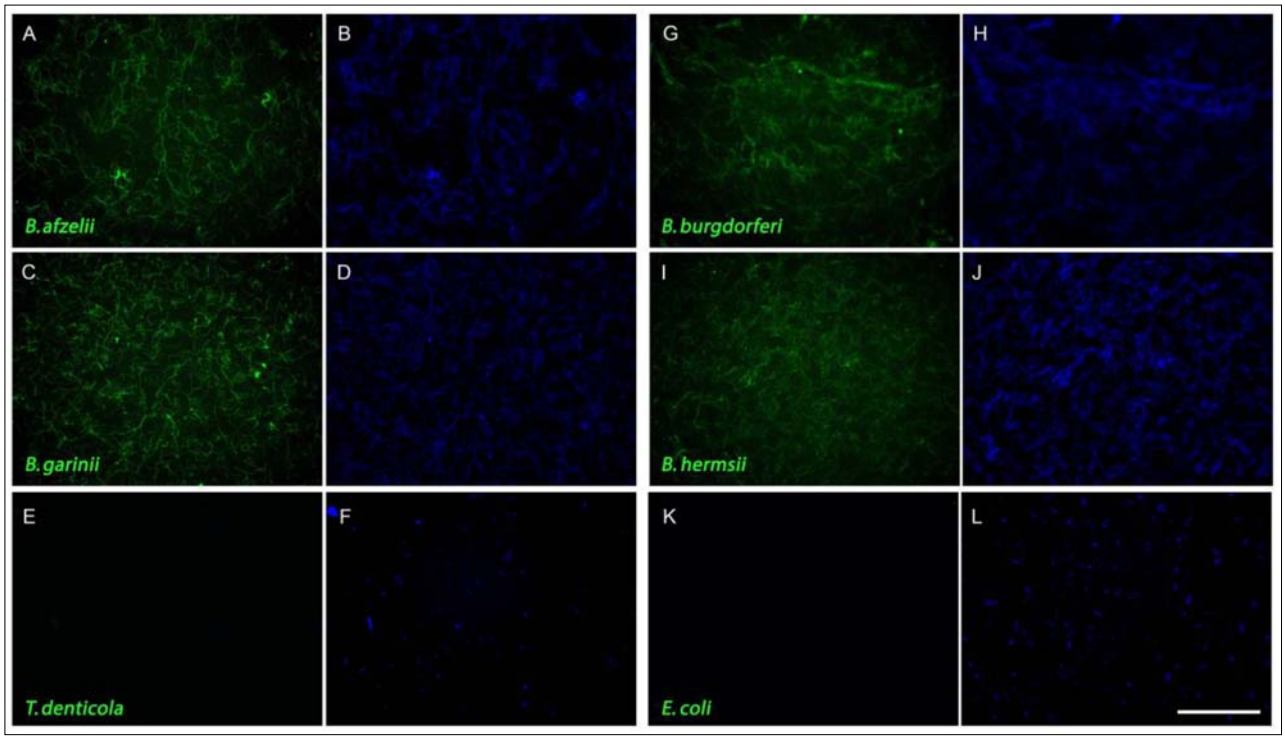

Fig. 3. A representative image shows a validation study for our 16S rDNA fluorescent *in situ* hybridization (FISH) protocol using different bacterial cells. The different bacterial cells placed on microscope slides and fixed and FISH protocols were carried out as described in Materials and methods section. The same FISH protocols were carried out on every experiment for *Borrelia afzelii* (panels A and B), *Borrelia garinii* (panels C and D), *Treponema denticola* (panels E and F), *Borrelia burgdorferi* (panels G and H), *Borrelia hermsii* (panels I and J), and *Escherichia coli* (panels K and L). DAPI nuclear stains depicting the cell morphology (panels B, D, F, H J, and L). 400× magnification, bar: 100 μm

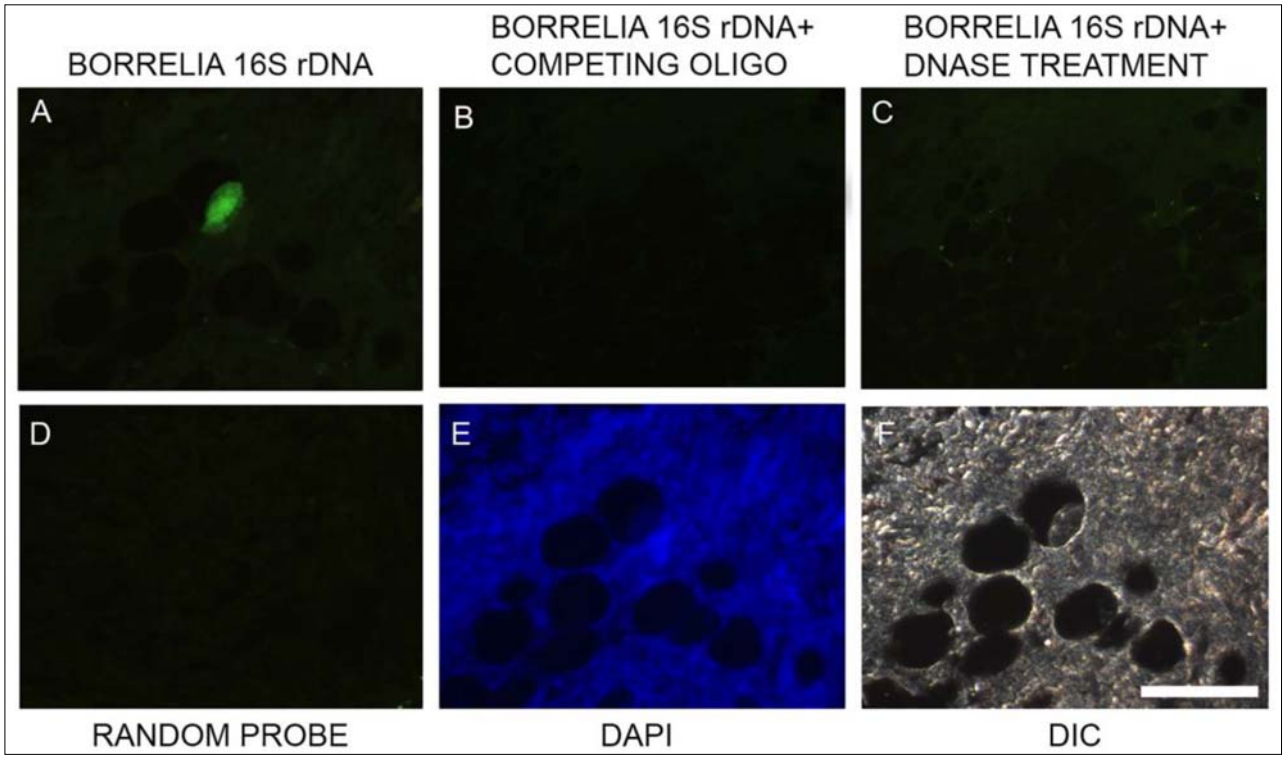

Fig. 4. Fluorescent *in situ* hybridization (FISH) of the BL tissues. *Borrelia*-specific 16S rDNA probe was utilized in these experiments to localize *Borrelia* DNA (A). As comprehensive negative controls, a competing oligonucleotide (B), DNase-treated samples (C), and a random DNA probe (D) were used on consecutive tissue sections to further show the specificity of the 16S rDNA probe (further details of the experimental conditions are in Materials and methods section). The tissue morphology was demonstrated with DAPI nuclear (E) and differential interphase contrast microscopy (DIC, panel F). 400× magnification, bar: 200 μm

staining) on the consecutive slide. *Figure 2*, panel Bviii, is a differential interference contract microscopy (DIC) image of *Fig. 2*, panel Bvii, demonstrating that there is still *Borrelia* aggregate on the slide despite the absence of staining.

Fluorescence in situ *hybridization (FISH) and PCR further prove* Borrelia *DNA presence in BL tissues*

To further confirm that the silver-stained aggregates observed in the BL tissues are indeed borrelial aggregates, we performed FISH experiments using a *B. burgdorferi sensu lato*-specific 16S rDNA probe. The specificity of our *in situ* hybridization method was first confirmed using commercially available laboratory strains for *B. burgdorferi*, *B. garinii*, *B. afzelii*, *B. hermsii*, *T. denticola*, and *E. coli* (see Materials and methods section). *Figure 3* shows that all *Borrelia* species stained positive while non-*Borrelia* species such as *T. denticola* and *E. coli* were found negative for *Borrelia*-specific DNA probe.

After validation of the experimental conditions with laboratory strains, we have used this *Borrelia*-specific FISH protocol on BL tissues sections. *Figure 4* shows a representative image of the FISH experiments that demonstrates that an aggregate found in BL tissues was successfully hybridized with *Borrelia*-specific 16S rDNA probe without significant background noise (A). As comprehensive negative controls, a competing oligonucleotide (B), DNase-treated samples (C), and a random probe (D) experimental conditions were used on consecutive tissue sections to show the specificity of the 16S rDNA FISH probe. None of the negative control experimental conditions resulted in significant fluorescent signal, providing evidence that the FISH experimental procedure is specific for *Borrelia* DNA.

Further validation of the presence of *Borrelia* spp. in the BL tissue biopsies was provided by extracting the genomic DNA and amplifying *B. burgdorferi sensu lato*-specific16S rDNA. Genomic DNA extracted from a *B. afzelii* laboratory strain (BO23) was used as a positive control, and no template control was used as negative controls. *Figure 5* demonstrates the result of the PCR experiments demonstrating the expected PCR bands in both the DNA extracted from the BL skin sections (S1–S6) as well as in the laboratory strain positive control *(Fig. 5)*. No PCR products were seen in the no template samples (−C), thus eliminating the possibility of contamination and, therefore, a nonspecific amplification in the PCR reaction. All PCR products were sequenced and analyzed by the BLAST program (NCBI) and identified to have 99–100% identity to the *B. afzelii* 16S rDNA gene compared to the *B. afzelii K78* reference strain obtained from an Austrian cutaneous lesion, thus confirming the presence of *B. afzelii* DNA in our European BL biopsies.

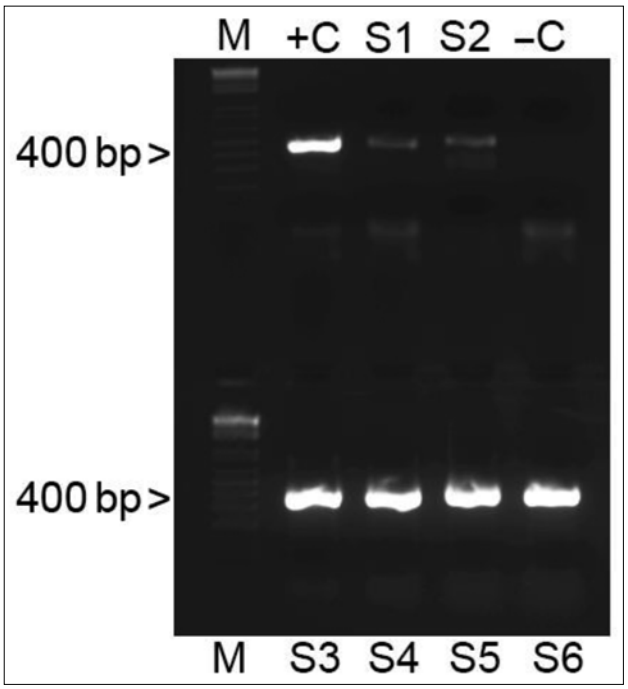

Fig. 5. Representative agarose gel picture of a *Borrelia burgdorferi sensu lato* specific 16S rDNA PCR amplification of genomic DNAs obtained from borrelial lymphocytoma skin sections. Lane M: 1 kb DNA Ladder (Life Technologies). Genomic DNA extracted from *Borrelia afzelii* laboratory strain (positive control, +C) and no template negative control (−C). Genomic DNAs extracted from borrelial lymphocytoma skin sections located in the S1–S6 lanes. The bands seen in lanes of +C and S1–S6 (~450 bp) represent DNA amplified using *Borrelia*-specific primers which have a target size of 445 bp, indicating the presence of *Borrelia burgdorferi sensu lato* DNA in the samples. No bands were seen in the negative control (−C)

Presence of biofilm markers associated with the aggregates in BL tissues

Having conclusively demonstrated the presence of *Borrelia* spirochetes and aggregates in BL tissues, we next asked whether the *Borrelia*-positive aggregates found in the BL tissue are biofilms. A hallmark characteristic of biofilms is the presence of extracellular polysaccharides which play major roles in protection, immune evasion, and antibiotic resistance. We had previously shown that the biofilms formed by various *Borrelia* species are rich in mucopolysaccharides and share similarities with biofilms formed by other bacteria [32–39]. We characterized the presence of mucopolysaccharides using an adaptation of the Spicer & Meyer aldehyde fuchsine–alcian blue sequential staining method (see Materials and methods section), which can differentiate between sulfated and non-sulfated/carboxylated mucins. Fuchsia/purple coloration indicates sulfated mucins while blue coloration indicates non-sulfated/carboxylated mucins. Results of this staining method show that *Borrelia*-positive aggregates in BL biopsies have similar staining pattern to the *in vitro Borrelia* aggregates found previously [30] staining for both sulfated (fuchsia/purple) and non-sulfated (blue) mucins.

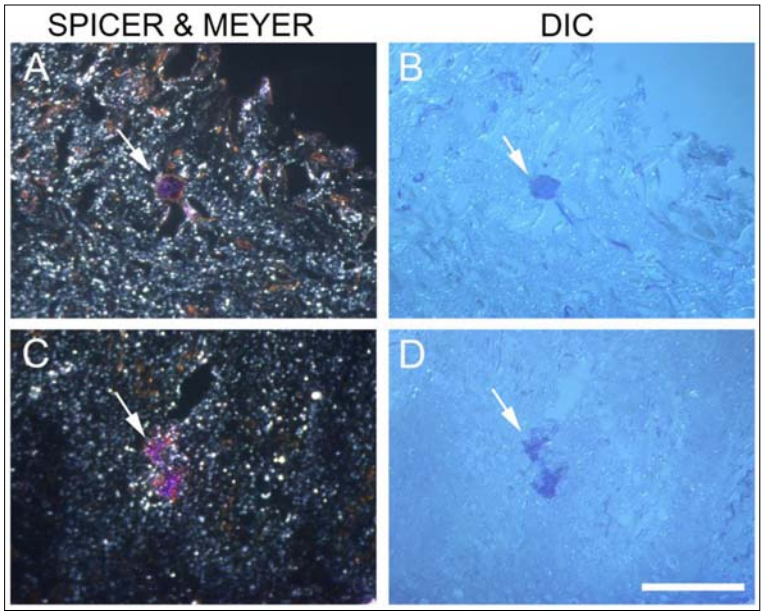

Fig. 6. Representative images showing Spicer & Meyer aldehyde fuchsine–alcian blue sequential staining pattern of two aggregates (white arrows) found in the BL tissues via dark field (panels A and C) and by differential interference contrast (panels B and D) microscopy methods. Fuchsia/purple colorations are indicative of sulfomucins and blue coloration indicates non-sulfated, carboxylated mucins. 400× magnification, bar: 200 μm

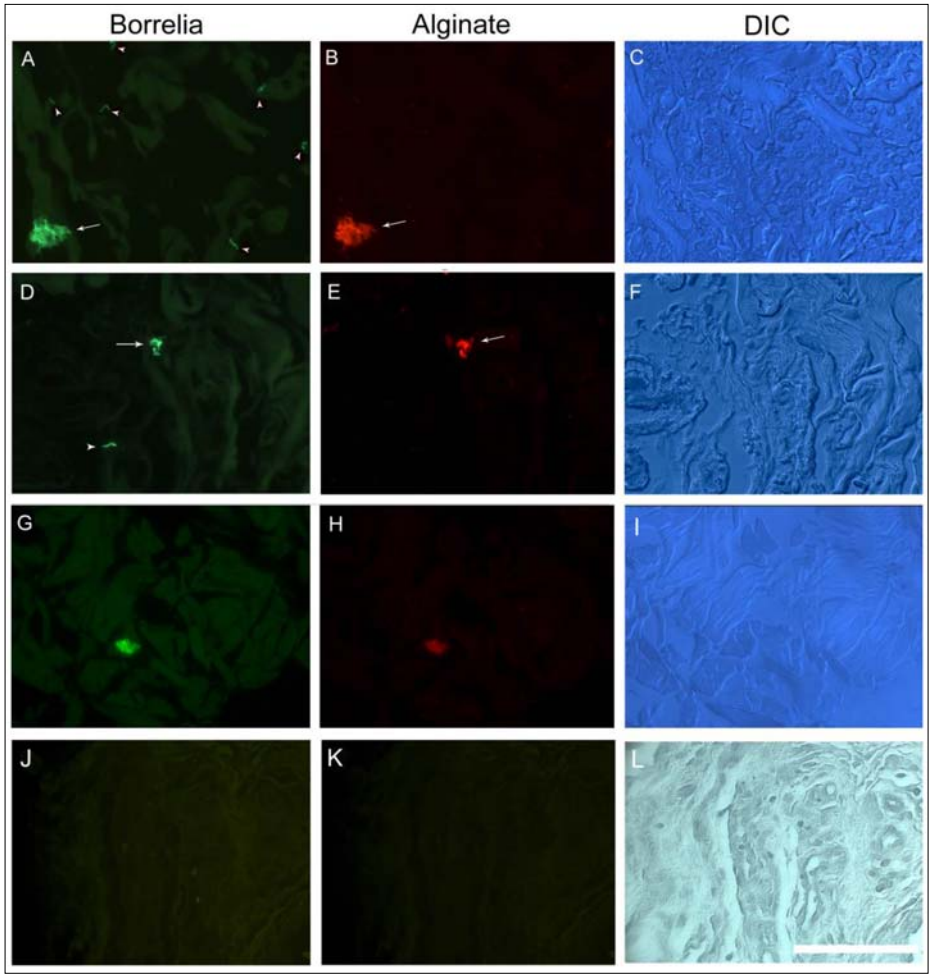

Fig. 7. Representative images of IHC analyses of spirochetes and aggregates found in BL tissues costained with *Borrelia* (green) and alginate (red) antibodies on the same tissue sections (panels A and B as well as D and E) or consecutive tissue section (panels G and H). As negative control, the same IHC experiments were repeated on normal foreskin tissue sections (panels J and K). Differential interference contrast (DIC) images were provided to show the morphology of the tissues (panels C, F, I, and L). 400× magnification, bar: 200 μm

Figure 6 shows the Spicer & Meyer staining pattern of two representative aggregates (white arrows) found in the BL biopsies by dark field *(Fig. 6A and C)* and DIC microscopy methods (*Fig. 6B* and *D*). The images depicting all three colors: fuchsia, purple, and blue indicate various mucopolysaccharides with different chemical composition on the surface of *Borrelia* aggregates in the BL tissues**.**

Taken together, these results demonstrate that the aggregates found in BL tissues are *Borrelia*-positive by two independently performed IHC and FISH techniques and they do contain certain biofilm markers such as mucopolysaccharides on their surfaces. The blue coloration on the surface of the aggregates indicated non-sulfated mucins which strongly suggested alginate presence similarly to what we found on the surface of *in vitro Borrelia* biofilms.

Borrelia *aggregates, but not spirochetes, strongly express alginates*

In the following experiments, the goal was to confirm that *Borrelia* aggregates indeed have alginate on their surfaces, by different immunostaining methods using *Borrelia*- and alginate-specific antibodies. Alginate antibody used in this study was validated in our previous *in vitro* studies showing that it does not stain individual *Borrelia* spirochetes as well as certain *E. coli* biofilms [30, 39]. As additional independent control, we have also used 20 commercially purchased normal human foreskin sections. *Figure 7* shows representative images of BL sections positively costained with both *Borrelia*- and alginate-specific antibodies (*Fig. 7A–B* and *D–E*). We also repeated the double staining experiments on consecutive slides using *Borrelia* and alginate antibodies to demonstrate independent *Borrelia* and alginate stainings on the same biofilm (*Fig. 7G* and *H*).

To further prove that the primary *Borrelia*- and alginate-specific antibodies do not have unspecific staining on human skin tissue, we have repeated the above experiments on human foreskin sections (*Fig. 7J* and *K*). Also, all individual spirochetes (*Fig. 7A* and *D;* white arrowheads) were all alginate negative (*Fig. 7B* and *E*), a result, which further demonstrates that alginate is specific to *Borrelia* aggregates and the two antibodies used in these experiments do not cross-react.

In the next experiments, we repeated the IHC experiments with *Borrelia*- and alginate-specific antibodies using 1200 sections (200 sections/specimen). While the majority of the sections contained at least one *Borrelia* immunopositive spirochete (none of them stained for alginate), only ~5% of all the sections contained *Borrelia*-positive aggregates with all different sizes. *Figure 8* represents a summary graph of the number of the spirochetes (ranging from 350 to 480 spirochetes/200 sections/specimen) and the number of aggregates (ranging from 4 to 12 aggregates/200 sections/specimen) observed in the six BL tissues (BL1-BL6) as well as in the commercially purchased normal human foreskin tissue specimens (control). There were no detectable *Borrelia*-positive spirochetes or aggregates found in any of the control specimens. Statistical analyses of the number of spirochetes or aggregates detected in the six BL tissues showed no significant differences among the specimens (p values >0.05).

IHC findings demonstrated that every *Borrelia* aggregate, but not any of the observed spirochete, was also posi-

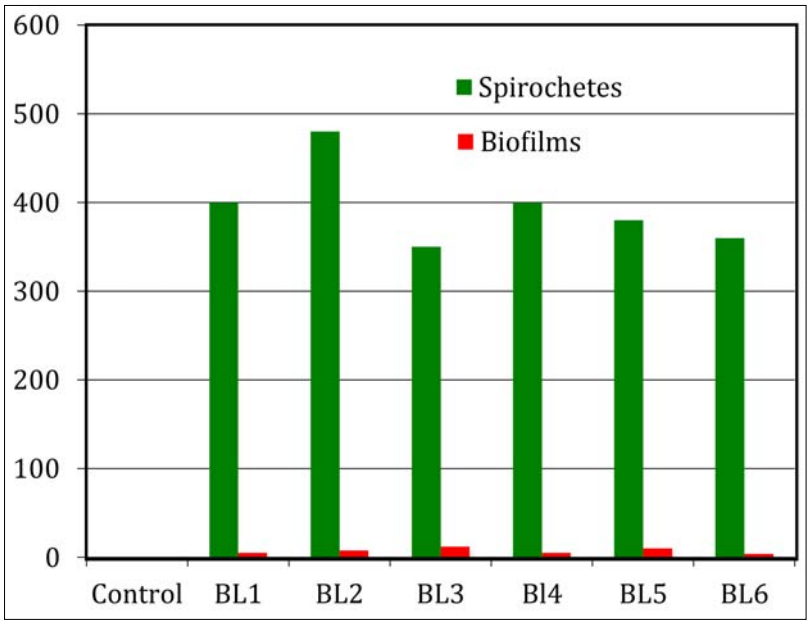

Fig. 8. Graphical representation of the number of the spirochetes and the number of aggregates observed in 1200 sections of six BL tissues (BL1-BL6; 200 sections/specimen) as well as in commercially purchased normal human foreskin tissue specimens (20 specimens). *Y*-axes data shows the number of the spirochetes (ranging from 350 to 480 spirochetes/200 sections/specimen) and the number of aggregates (ranging from 4 to 12 aggregates/200 sections/specimen) found in the six BL tissue. There were no detectable spirochetes or aggregates found in any of the control specimens

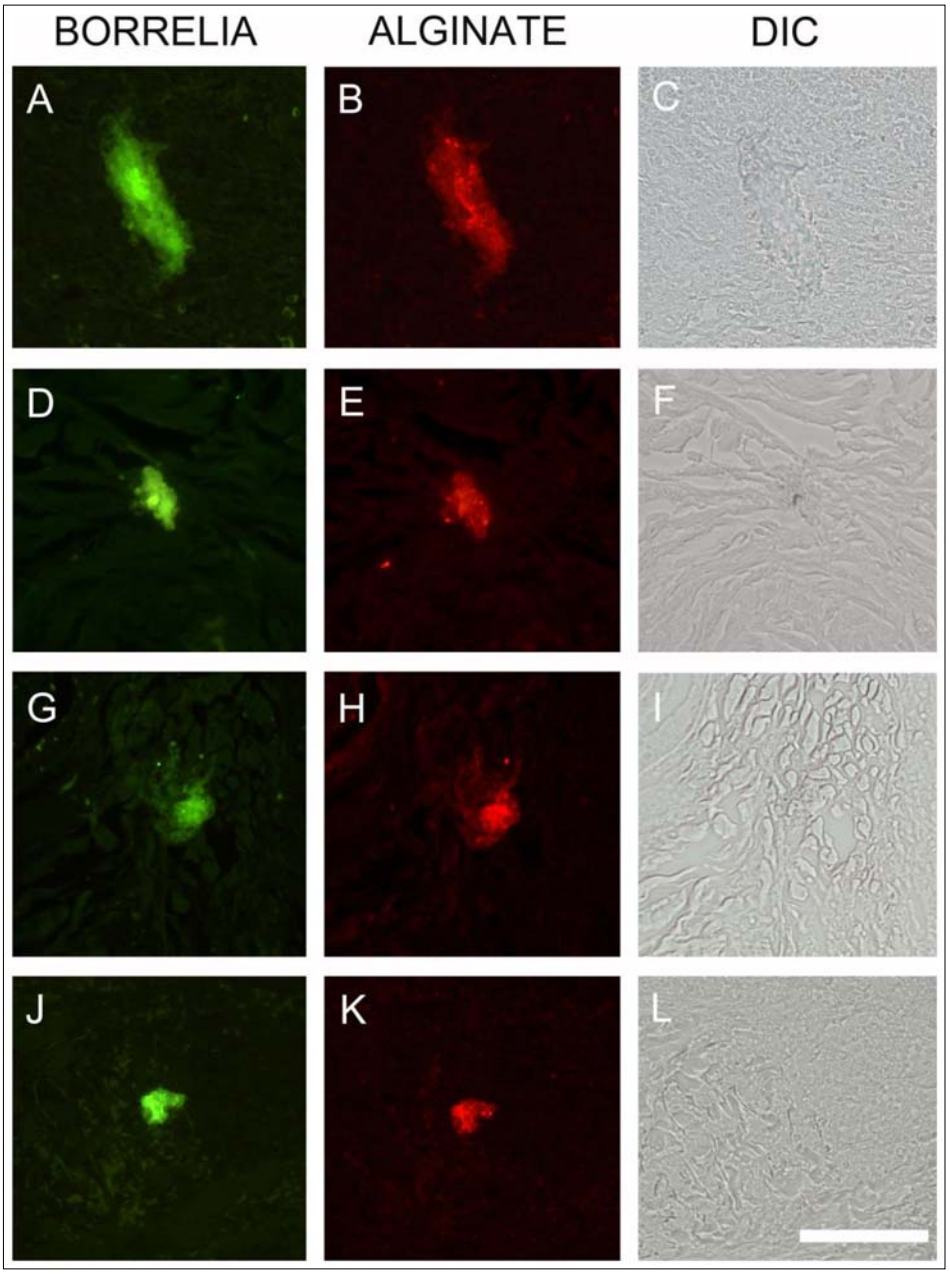

Fig. 9. Immunohistochemical staining of BL skin sections showing several different aggregates stained positive with *Borrelia* (green staining: panels A, D, G, and J) and alginate specific antibodies (red staining: panels B, E, H and K). Differential interference microscopy (DIC) showing the size and tissue morphology of the skin tissues (panels C, F, I, and L). 400× magnification, bar: 200 μm

tive for alginate. Very importantly, nonspecific alginate staining was not observed anywhere else in the BL skin tissues. *Figure 9* shows the heterogeneity in sizes of *Borrelia* aggregates in BL biopsies which were positive for both *Borrelia* and alginate antigens.

Merged images show the localization of alginate associated with *Borrelia*-positive aggregates in sections which were dual stained with both anti-*Borrelia* (green) and anti-alginate (red) antibodies (*Fig. 10,* panels v and vi). The yellow colored regions in the merged figures show regions, which contain both *Borrelia* and alginate antigens. Bright field images showing the skin tissue stained with Sudan black B (*Fig. 10,* panels vii and viii) show the size and morphology of the skin tissue.

Combined FISH and IHC experiments further provide evidence that Borrelia *aggregates indeed express alginate on their surfaces*

Alternatively, the expression of alginate on the surface of *Borrelia*-positive aggregates in BL skin tissues was also detected using a combined FISH and IHC experiments with 16S rDNA probe for *Borrelia* detection and alginate antibody for alginate antigen detection. *Figure 11* shows a representative image which shows that a *Borrelia*-specific FISH positive structure (A) stains for alginate (B) as well as detected by IHC method. As a negative control, a competing oligonucleotide FISH was included to demonstrate the specificity of the *Borrelia* FISH DNA probe (C).

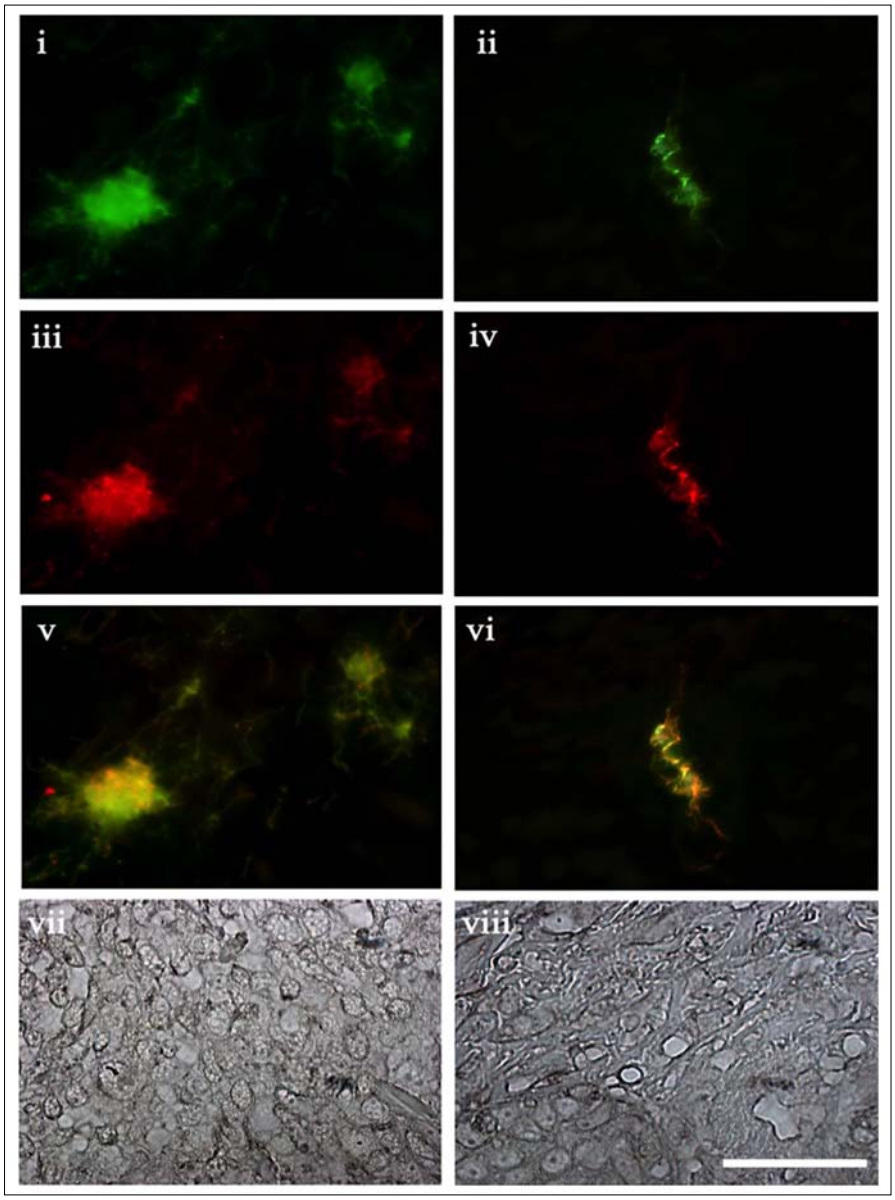

Fig. 10. IHC staining of BL skin sections showing two different aggregates stained positive with *Borrelia* antigen (green staining: panels i and ii) and alginate (red staining: panels iii and iv). Panels v and vi are a merge of the anti-*Borrelia* and anti-alginate antibody. Panels vii and viii show the bright field image with Sudan Black-B staining. In the merged picture, yellow/light orange indicates the regions where both *Borrelia* and alginate are present. 1000× magnification, bar: 200 μm

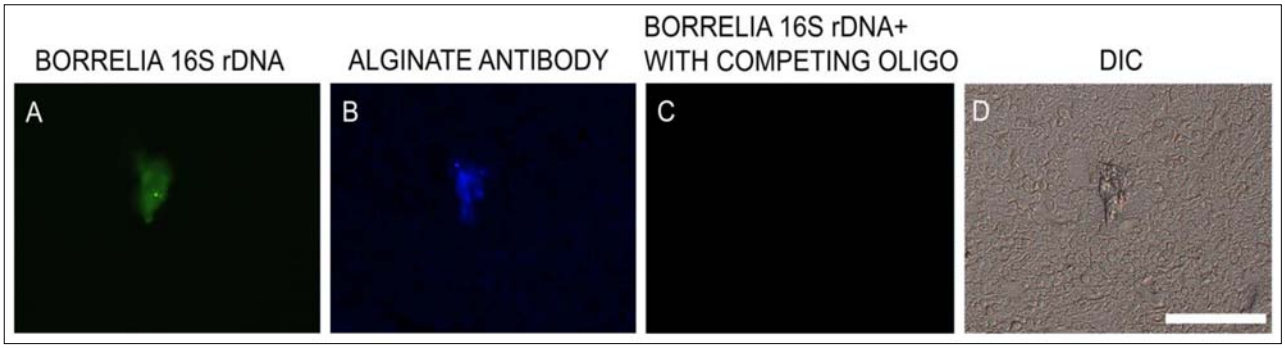

Fig. 11. Combined FISH and IHC representative image of *Borrelia* aggregates in BL skin tissues showing that *Borrelia*-DNA-positive structures identified with FISH experiment using 16S rDNA probe (green staining, panel A) express alginate antibody (blue staining, panel B) as depicted with an independent IHC method. To show that the structure indeed is *Borrelia* DNA positive, competing oligonucleotide was used as a negative control (panel C). Differential interference microscopy (DIC) showing the size and tissue morphology of the skin tissues (panel D). 400× magnification, bar: 200 μm

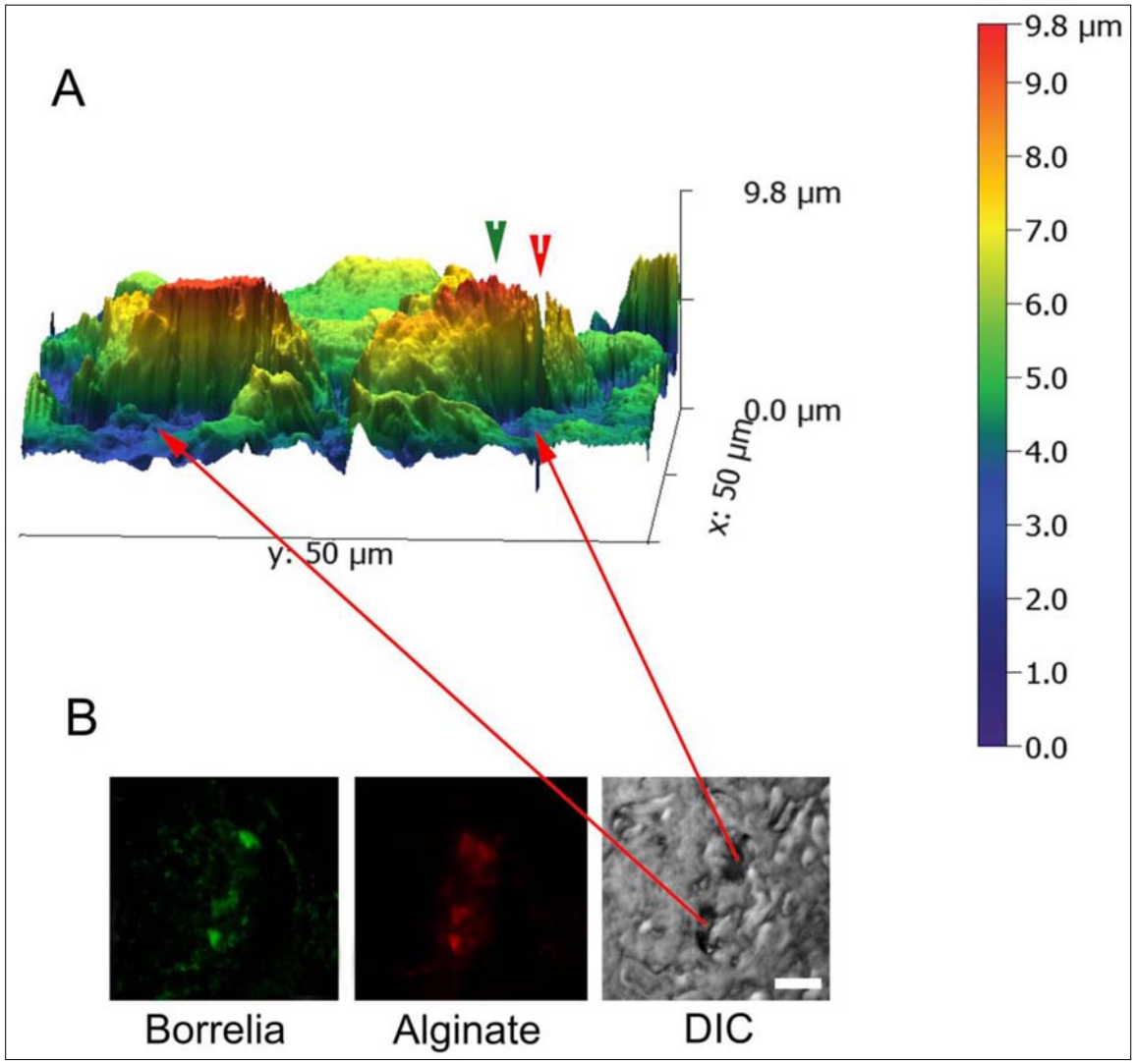

Fig. 12. Three-dimensional atomic force microscopy analyses of *Borrelia*/alginate-positive aggregates from a BL biopsy tissue section. Panel A shows a representative image from the AFM analyses which was performed using contact mode of the Nanosurf Easyscan 2 AFM with SHOCONG probe (AppNANO™ [30]). Images were processed, and measurements were obtained using Gwyddion software. The individual height and width ranges are indicated on the panels. Panel B shows evidence that the scanned tissue is *Borrelia*- and alginate-positive by fluorescent IHC analyses (400× magnification). Red arrows represent the same area of the tissue illustrated on panels A and B. Red and green arrowheads indicate potential channels and protrusions in the *Borrelia*/alginate-positive aggregates, bar: 200 µm

Ultra structural analysis of the Borrelia- *and alginate-positive aggregates in BL biopsies by atomic force microscopy (AFM)*

Finally, to understand the ultrastructural organization of *Borrelia* and alginate dual positive aggregates, we performed atomic force microscopy. *Figure 12* shows representative micrographs of a dual stained *Borrelia* aggregate costained with both *Borrelia*- and alginate-specific antibodies, which is deeply embedded in the surrounding tissues, observed using DIC microscopy *(Fig. 12B)*. AFM topographical scans also confirmed that the aggregates are indeed embedded in the tissues (indicated by the red arrows) and have the characteristic channels and protrusions that we observed in the *in vitro Borrelia* biofilms (red and green arrowheads respectively) *(Fig. 12A)*.

Discussion

We have previously provided evidence that *B. burgdorferi sensu stricto* and *sensu lato*, the Lyme disease causing spirochete bacteria, are capable of forming biofilms *in vitro* [30, 38]. The goal of this study was to find and characterize potential *Borrelia* biofilms *in vivo* using infected skin tissues of BL biopsies from Austrian Lyme disease patients. Our findings demonstrated that the observed aggregates are indeed *Borrelia*-positive structures that express specific biofilm markers such as sulfated and non-sulfated mucopolysaccharides which are mainly alginate. Our data also demonstrated that the observed *Borrelia*-positive spirochetes do not express alginate which further support the hypothesis that those *Borrelia*-positive aggregates are indeed biofilm structures. Our AFM studies further charac-

terized the ultrastructure of *Borrelia*- and alginate-positive aggregates and found additional biofilm characteristic properties such as channels and protrusions of the tissue-embedded biofilms.

Human biopsies used in this study were lesions from BL from Lyme disease patients, a skin condition known for the presence of *Borrelia* spirochetes and reported mainly from Europe [42].

BL biopsies were previously analyzed for the different morphological forms of *Borrelia* through focus-floating microscopy methods [41]. Findings from this study revealed the presence of *Borrelia* spirochetes as clusters of granular colonies. These descriptions are consistent with an aggregate of organisms enmeshed in a matrix, similar to the *Borrelia* biofilm found *in vitro* [30, 38]. To determine whether the *Borrelia* aggregates described in BL biopsies are indeed biofilms, BL biopsy tissues from the same archive collection were reexamined for biofilm-specific markers. Our results on human BL biopsy sections first revealed the presence of *Borrelia* spirochetes and aggregates by *Borrelia*-specific IHC methods combined with additional silver staining, FISH techniques. To confirm the specificity of our techniques, we provided several independent negative controls for both the IHC and FISH experiments such as: 1) the samples were analyzed independently in European and in US laboratories respectively; 2) *Borrelia* and alginate IHC experiments were performed on the same and sequential slides; 3) use of uninfected human foreskin samples and no antibody control in the immunohistochemical experiments; 4) validation of our FISH experiments with borrelial and non-borrelial laboratory strains; 5) different *in situ* hybridization negative controls (competing oligonucleotide, random DNA probes, and DNase-treated samples); and 6) combined IHC–FISH experiments, which all provided evidence that the results are indeed specific and do not represent background tissue staining.

Our findings also suggested that those *Borrelia*-positive aggregates, but not spirochetes, have several classical features of biofilm structures because they were strongly positive for different mucopolysaccharides as well as for alginate, a negatively charged sugar polymer. *Pseudomonas aeruginosa*, the causative agent of cystic fibrosis, forms biofilms rich in alginate that confer it protection from the host immune system [33, 35, 45–47]. Studies further reported that these biofilms are very resistant to antibiotics and result in chronic inflammation and damage to cystic fibrosis lung tissues. In other studies, however, it was confirmed that even after the degradation of the alginate present on the biofilm surface, the gentamycin resistance of the biofilm was not affected [46]. This implies that alginate might not be the only reason for the resistance of biofilms and that there are other components which confer antibiotic resistance. The exact role of alginate presence on the surface on *Borrelia* aggregates in the infected skin tissues still needs to be determined as well as the other potential protective layers indicated by our Spicer & Meyer findings.

The presence of alginate on the *Borrelia*-positive structures in LB tissues also provides a good argument against the theory called “amber hypothesis” which hypothesizes that dead spirochetes and borrelial debris can persist in the tissue and cause chronic inflammation in Lyme disease patients [48, 49]. The authors of these studies argued against the idea of potential biofilm because the isolated *Borrelia* aggregates found in mouse skin tissues failed to grow *in vitro*. Culture negativity of biofilms from different pathogens is one of the cornerstone concepts for the behavior of true biofilms [50, 51] as it was shown in biofilms in culture-negative orthopedic and endocardiatic biofilm infections [51, 52] and therefore cannot be used to dismiss the idea that *Borrelia* can make biofilm *in vivo.*

Among the order Spirochaetales, biofilms from *T. denticola* and *Leptospira* spp. have already been reported in periodontal diseases and dental water systems, respectively [37, 53]. Further investigation of *T. denticola* biofilm development revealed that it could be achieved *in vitro* on fibronectin surfaces in a low-shear-force environment [54]. We also found that certain surfaces are preferable for *Borrelia* biofilm formation *in vitro* such as collagen and fibronectin surfaces [30, 38], which correlates well with the results from this study where *Borrelia* aggregates were found in collagen- and fibronectin-rich skin tissues. Our differential interference contrast and atomic force microscopy data also showed that the *Borrelia* biofilms embedded deeply in the tissue suggesting a potential host tissue rearrangement during biofilm growth. The exact mechanism of host tissue remodeling during the dissemination of *B. burgdorferi* is under active investigation and suggests the use of a variety of bacterial factors and host enzymes; therefore, it is very likely that those *Borrelia* aggregates could use the same mechanism to embed the biofilm in the tissues and further protect the structure from the host defense. Findings from this study could also raise the question about the kind of other tissues that could be potential target for these *Borrelia* biofilm structures. In one of our ongoing mouse studies, we have analyzed multiple tissue sites in *Borrelia*-infected Balb/c mice model and found in multiple tissues with similar *Borrelia*-positive aggregates with alginate presence [55]. We are also in the process studying the molecular mechanism of the antibiotic resistance of *Borrelia* aggregates using different *Borrelia* mutant cell lines and identified important pathways which might be responsible for the observed resistance. For example, Lux S quorum sensing deficient *Borrelia* mutant showed incomplete biofilm development and reduced resistance against certain antibiotics, a result which agrees with the potential function of Lux S pathway during mammalian infection [56, 57].

In summary, in this study, we provided several lines of evidence that *Borrelia* biofilm could exist *in vivo*. Further confirmation and characterization of the presence of biofilm *in vivo* would help us better understand the survival strategies of the *Borrelia* spp. within its host and would provide important clinical data for therapeutic intervention for Lyme disease patients.

Acknowledgements

The authors would like to thank Dr. Gerald B. Pier (Harvard University) for the anti-alginate antibody and Dr. Tom G. Schwan (Rocky Mountain Laboratory) for *B. hermsii* cells used in this study. We also would like thank Joel Israel (McClain Histopathology Laboratory) for the silver staining experiments. This work was supported by grants from the University of New Haven, Lymedisease.org, Tom Crawford's Leadership Children Foundation, National Philanthropic Trust, Alyssa Wartman Funds to E.S., and postgraduate fellowships from NH Charitable Foundation to P.A.S.T. and K.M.S. We also thank the Lymedisease.org, the Schwartz Research Foundation for the donation of the Atomic Force and the Leica DM2500 microscopes as well as the Hamamatsu ORCA Digital Camera and the Global Lyme Alliance for the AFM supporting computer.

Competing interests

The authors have declared that no competing interest exists.

References

1. Barbour AG, Hayes SF: Biology of *Borrelia* species. Microbiol Rev 50, 381–400 (1986)
2. Mead, PS: Epidemiology of Lyme Disease. Infect Dis Clin North Am 29, 187–210 (2015)
3. Liegner KB, Shapiro JR, Ramsay D, Halperin AJ, Hogrefe W, Kong L: Recurrent erythema migrans despite extended antibiotic treatment with minocycline in a patient with persisting *Borrelia burgdorferi* infection. J Am Acad Dermatol 28, 312–314 (1993)
4. Dumler JS: Molecular diagnosis of Lyme disease: review and meta-analysis. Mol Diagn 6, 1–11 (2001)
5. Klempner MS, Baker PJ, Shapiro ED, Marques A, Dattwyler RJ, Halperin JJ, Wormser GP: Treatment trials for post-lyme disease symptoms revisited. Am J Med 126, 665–669 (2013)
6. Steere AC, Angelis, SM: Therapy for Lyme arthritis: Strategies for the treatment of antibiotic-refractory arthritis. Arthritis Rheum 54, 3079–3086 (2006)
7. Berndtson K: Review of evidence for immune evasion and persistent infection in Lyme disease. Int J Gen Med 6, 291–306 (2013)
8. Kurtti TJ, Munderloh, UG, Johnson RC, Ahlstrand GG: Colony formation and morphology in *Borrelia burgdorferi*. J Clin Microbiol 25, 2054–2058 (1987)
9. Mursic VP, Wanner G, Reinhardt S, Wilske B, Busch U, Marget W: Formation and cultivation of *Borrelia burgdorferi* spheroplast-L-form variants. Infection 24, 218–226 (1996)
10. Brorson O, Brorson SH: *In vitro* conversion of *Borrelia burgdorferi* to cystic forms in spinal fluid, and transformation to mobile spirochetes by incubation in BSK-H medium. Infection 26, 144–150 (1998)
11. Hampp EG: Further studies on the significance of spirochetal granules. J Bacteriol 62, 347–349 (1951)
12. Alban PS, Johnson PW, Nelson DR: Serum-starvation-induced changes in protein synthesis and morphology of *Borrelia burgdorferi*. Microbiology 146, 119–127 (2000)
13. Gruntar I, Malovrh T, Murgia R, Cinco M: Conversion of *Borrelia garinii* cystic forms to motile spirochetes *in vivo*. APMIS 109, 383–388 (2001)
14. Murgia R, Cinco M: Induction of cystic forms by different stress conditions in *Borrelia burgdorferi*. APMIS 112, 57–62 (2004)
15. Brorson Ø, Brorson SH: An *in vitro* study of the susceptibility of mobile and cystic forms of *Borrelia burgdorferi* to tinidazole. Int Microbiol 7, 139–42 (2004)
16. MacDonald AB: Spirochetal cyst forms in neurodegenerative disorders,…hiding in plain sight. Med Hypotheses 67, 819–832 (2006)
17. Miklossy J, Kasas S, Zurn AD, McCall S, Yu S, McGeer PL: Persisting atypical and cystic forms of *Borrelia burgdorferi* and local inflammation in Lyme neuroborreliosis. J Neuroinflammation 5, 1–18 (2008)
18. Kersten A, Poitschek C, Rauch S, Aberer E: Effects of penicillin, ceftriaxone, and doxycycline on morphology of *Borrelia burgdorferi*. Antimicrob Agents Chemother 39, 1127–1133 (1995)
19. Brorson Ø, Brorson S-H, Scythes J, MacAllister J, Wier A, Margulis L: Destruction of spirochete *Borrelia burgdorferi* round-body propagules (RBs) by the antibiotic tigecycline. Proc Natl Acad Sci 106, 18656–18661 (2009)
20. Sapi E, Kaur N, Anyanwu S, Luecke DF, Datar A, Patel S, Rossi M, Stricker RB: Evaluation of *in vitro* antibiotic susceptibility of different morphological forms of *Borrelia burgdorferi*. Infect Drug Resist 4, 97–113 (2011)
21. Feng J, Wang T, Shi W, Zhang S, Sullivan D, Auwaerter PG Zhang Y: Identification of novel activity against *Borrelia burgdorferi* persisters using an FDA approved drug library. Emerg Microbes Infect 3, e49 (2014)
22. Feng J, Auwaerter PG, Zhang Y: Drug combinations against *Borrelia burgdorferi* persisters *in vitro*: eradication achieved by using daptomycin, cefoperazone and doxycycline. PLoS One 10, 1–15 (2015)
23. Straubinger RK, Summers, BA, Chang YF, Appel MJ: Persistence of *Borrelia burgdorferi* in experimentally infected dogs after antibiotic treatment. J Clin Microbiol 35, 111–116 (1997)
24. Hodzic E, Feng S, Holden K, Freet KJ, Barthold SW: Persistence of *Borrelia burgdorferi* following antibiotic treatment in mice. Antimicrob Agents Chemother 52, 1728–1736 (2008)
25. Barthold SW, Hodzic E, Imai DM, Feng S, Yang S, Luft BJ: Ineffectiveness of tigecycline against persistent *Borrelia burgdorferi*. Antimicrob Agents Chemother 54, 643–651 (2010)
26. Embers ME, Barthold SW, Borda JT, Bowers L, Doyle L, Hodzic E, Jacobs MB, Hasenkampf NR, Martin DS, Narasimhan S, Phillippi-Falkenstein KM, Purcell JE, Ratterree MS, Philipp MT: Persistence of *Borrelia burgdorferi* in rhesus macaques following antibiotic treatment of disseminated infection. PLoS One 7, e29914 (2012)
27. Hodzic E, Imai D, Feng S, Barthold SW: Resurgence of persisting non-cultivable *Borrelia burgdorferi* following antibiotic treatment in mice. PLoS One 23, 1–11 (2014)
28. Costerton, JW, Stewart, PS, Greenberg, EP: Bacterial biofilms: a common cause of persistent infections. Science 284, 1318–1322 (1999)

29. Donlan RM, Costerton JW: Biofilms: Survival mechanisms of clinically relevant microorganisms. Clin Microbiol Rev 15, 167–93 (2002)
30. Sapi E, Bastian SL, Mpoy CM, Scott S, Rattelle A, Pabbati N, Poruri A, Burugu D, Theophilus PA, Pham TV, Datar A, Dhaliwal NK, MacDonald A, Rossi MJ, Sinha SK, Luecke DF: Characterization of biofilm formation by *Borrelia burgdorferi in vitro.* PLoS One 7, e48277 (2012)
31. Fitzpatrick F, Humphreys H, O'Gara JP: Environmental regulation of biofilm development in methicillin-resistant and methicillin-susceptible *Staphylococcus aureus* clinical isolates. J Hosp Infect 62, 120–122 (2006)
32. Dordel J, Kim C, Chung M, Pardos de la Gándara M, Holden MT, Parkhill J, de Lencastre H, Bentley SD, Tomasz A: Novel determinants of antibiotic resistance: identification of mutated loci in highly methicillin-resistant subpopulations of methicillin-resistant *Staphylococcus aureus.* MBio 5, e01000 (2014)
33. Clementi, F: Alginate production by *Azotobacter vinelandii*. Crit Rev Biotechnol 17, 327–361 (1997)
34. Hentzer M, Teitzel GM, Balzer GJ, Heydorn A, Molin S, Givskov M, Parsek MR: Alginate overproduction affects *Pseudomonas aeruginosa* biofilm structure and function. J Bacteriol 183, 5395–5401 (2001)
35. Branda SS, Vik Å, Friedman L, Kolter R: Biofilms: the matrix revisited. Trends Microbiol 13, 20–26 (2005)
36. Allesen-Holm M, Barken KB, Yang L, Klausen M, Webb JS, Kjelleber S, Molin S, Givskov M, Tolker-Nielsen T: A characterization of DNA release in *Pseudomonas aeruginosa* cultures and biofilms. Mol Microbiol 59, 1114–1128 (2006)
37. Ristow P, Bourhy P, Kerneis S, Schmitt C, Prevost MC, Lilenbaum W, Picardeau M: Biofilm formation by saprophytic and pathogenic leptospires. Microbiology 154, 1309–1317 (2008)
38. Timmaraju VA, Theophilus PAS, Balasubramanian K, Shakih S, Luecke DF, Sapi E: Biofilm formation by *Borrelia sensu lato.* FEMS Microbiol Lett 362, fnv120 (2015)
39. Remminghorst U, Rehm BHA: Bacterial alginates: from biosynthesis to applications. Biotechnol Lett 28, 1701–1712 (2006)
40. Sharma B, Brown A V., Matluck NE, Hu LT, Lewis K: *Borrelia burgdorferi*, the causative agent of Lyme disease, forms drug-tolerant persister cells. Antimicrob Agents Chemother 59, 4616–4624 (2015)
41. Eisendle K, Grabner T, Zelger B: Focus floating microscopy: "Gold Standard" for cutaneous Borreliosis? Am J Clin Pathol 127, 213–222 (2007)
42. Eisendle K, Zelger B: The expanding spectrum of cutaneous borreliosis. G Ital Dermatol Venereol 144, 157–171 (2009)
43. Duray P, Kusnitz A, Ryan J: Demonstration of the Lyme disease spirochete by a modified Dieterle stain method. Lab Med 16: 685–687 (1985)
44. Schüler W, Bunikis I, Weber-Lehman J, Comstedt P, Kutschan-Bunikis S, Stanek G, Huber J, Meinke A, Bergström S, Lundberg U: Complete genome sequence of *Borrelia afzelii* K78 and comparative genome analysis. PLoS One 10, e0120548 (2015)
45. Høiby N, Ciofu O, Bjarnsholt T: *Pseudomonas aeruginosa* biofilms in cystic fibrosis. Future Microbiol 5, 1663–1674 (2010)
46. Stapper AP: Alginate production affects *Pseudomonas aeruginosa* biofilm development and architecture, but is not essential for biofilm formation. J Med Microbiol 53, 679–690. (2004)
47. Aspe M, Jensen L: The role of alginate and extracellular DNA in biofilm-meditated *Pseudomonas aeruginosa* gentamicin resistance. J Exp Microbiol Immunol 16, 42–48. (2012)
48. Wormser JP, Nadelman RB, Schwartz I: The amber theory of Lyme arthritis: initial description and clinical implications**.** Clin Rheumatol 31, 989–994 (2012)
49. Bockenstedt, LK, Gonzales DG, Haberman AM, Belperron AA: Spirochete antigens persist near cartilage after murine Lyme borreliosis therapy. J Clin Invest 122, 2652–2660 (2012)
50. Lynch JF, Lappin-Scott HM, Costerton JW (2003): Microbial Biofilms, Cambridge University Press, Cambridge, UK
51. Ehrlich GD, DeMeo PJ, Costerton JW, Winkler H (eds.): Culture negative orthopedic biofilm infections. In: Springer Series on Biofilms, Springer-Yerlag, Berlin Heidelberg, pp. 1–28
52. Baddour LM, Freeman WK, Suri RM, Wilson WR (2014): Cardiovascular infections. In: Braunwald's Heart Disease: A Textbook of Cardiovascular Medicine, eds. Mann DL, Zipes DP, Libby P, Bonow RO, Braunwald E, Elsevier Saunders: Philadelphia, PA, Chapter 64
53. Singh R, Stine OC, Smith DL, Spitznagel JK Jr, Labib ME, Williams HN: Microbial diversity of biofilms in dental unit water systems. Appl Environ Microbiol 69, 3412–3420 (2003)
54. Vesey PM: Genetic analysis of *Treponema denticola* ATCC 35405 biofilm formation. Microbiology 150, 2401–2407 (2004)
55. Balasubramanian K: Evidence for the presence of *Borrelia burgdorferi* biofilm in infected human and mouse tissues. Master Thesis. University of New Haven, Department of Biology and Environmental Science (2015)
56. Stevenson B, Babb K: LuxS-mediated quorum sensing in *Borrelia burgdorferi*, the Lyme disease spirochete. Infect Immun 70, 4099–4105 (2002)
57. Mpoy CM: Expression profile of quorum sensing biomarkers during biofilm development of *Borrelia burgdorferi.* Master Thesis. University of New Haven, Department of Biology and Environmental Science (2012)